Chiral Spin Liquids in Triangular-Lattice SU(N) Fermionic Mott Insulators with Artificial Gauge Fields

Pierre Nataf,[1] Miklós Lajkó,[2] Alexander Wietek,[3] Karlo Penc,[4,5] Frédéric Mila,[1] and Andreas M. Läuchli[3]
[1]Institute of Physics, Ecole Polytechnique Fédérale de Lausanne (EPFL), CH-1015 Lausanne, Switzerland
[2]Institute for Solid State Physics, University of Tokyo, Kashiwa 277-8581, Japan
[3]Institut für Theoretische Physik, Universität Innsbruck, A-6020 Innsbruck, Austria
[4]Institute for Solid State Physics and Optics, Wigner Research Centre for Physics, Hungarian Academy of Sciences, H-1525 Budapest, P.O.B. 49, Hungary
[5]MTA-BME Lendület Magneto-optical Spectroscopy Research Group, 1111 Budapest, Hungary
(Received 29 January 2016; published 11 October 2016)

We show that, in the presence of a $\pi/2$ artificial gauge field per plaquette, Mott insulating phases of ultracold fermions with SU(N) symmetry and one particle per site generically possess an extended chiral phase with intrinsic topological order characterized by an approximate ground space of N low-lying singlets for periodic boundary conditions, and by chiral edge states described by the $\mathrm{SU}(N)_1$ Wess-Zumino-Novikov-Witten conformal field theory for open boundary conditions. This has been achieved by extensive exact diagonalizations for N between 3 and 9, and by a parton construction based on a set of N Gutzwiller projected fermionic wave functions with flux π/N per triangular plaquette. Experimental implications are briefly discussed.

DOI: 10.1103/PhysRevLett.117.167202

The search for unconventional quantum states of matter in realistic models of strongly correlated systems has been an extremely active field of research over the last 25 years. Mott insulating phases in which charge degrees of freedom are gapped have been argued to potentially host several families of quantum spin liquids ranging from resonating valence bond $\mathbb{Z}_2$ quantum spin liquids [1–3] to U(1) algebraic spin liquids [4–6] and chiral spin liquids (CSLs) [7–15]. The topological properties of these phases have attracted a lot of attention due to their potential impact on the implementation of quantum computers [16].

Cold atoms open new perspectives in that respect. In particular, alkaline rare earths allow one to realize SU(N) Mott phases with N as large as 10 [17–24], and if a chiral phase can be stabilized, its low-energy theory is expected to be the SU(N) level $k = 1$ Chern-Simons theory. The possibility to destroy long-range order in SU(N) generalizations of the SU(2) antiferromagnet on bipartite lattices has long been known [4,25], but the first proposal of a chiral phase in the context of SU(N) models of cold atoms goes back to the work of Hermele *et al.* [26,27], who showed that a mean-field approach leads to the stabilization of chiral phases on the square lattice in the limit of large N and a large number of particles per site m with N/m integer and ≥ 5. The same mean field applied to $SU(6)$ on the honeycomb lattice with one particle per site has also led to the prediction of a chiral state, with a competing plaquette state very close in energy [28]. More recently, Ref. [29] suggested the stabilization of SU(N) CSLs on the square lattice using static synthetic gauge fields, based on a slave-rotor mean-field approach. In all theses cases, the results call for further investigation with methods that go beyond mean-field theory.

In this Letter, we show that the ground state of the Mott phase of N-color fermions on the triangular lattice with one particle per site is a SU(N) CSL in a large parameter range if the system is subject to a static artificial gauge field with flux $\pi/2$ per triangular plaquette. The starting point is the SU(N) Hubbard Hamiltonian

$$H = -t\sum_{\langle i,j\rangle}\sum_{\alpha=1}^{N}(e^{\phi_{ij}}c^{\dagger}_{i,\alpha}c_{j,\alpha} + \mathrm{H.c.}) + U\sum_{i,\alpha<\beta} n_{i,\alpha}n_{i_\beta}. \quad (1)$$

If the phases ϕ_{ij} are chosen in a such a way that the (gauge-invariant) flux through each triangular plaquette is equal to Φ, then, at a filling of one particle per site, and for large enough U/t, the effective model is an SU(N) Heisenberg model with local spins in the fundamental representation of SU(N) endowed with real pairwise permutations and complex three-site permutations. The Hamiltonian is a generalization of the SU(2) model with scalar chirality [30,31] and is defined by

$$H = J\sum_{\langle i,j\rangle} P_{ij} + K_3\sum_{(i,j,k)}(e^{i\Phi}P_{ijk} + \mathrm{H.c.}), \quad (2)$$

where the sum over (i,j,k) runs over all triangular plaquettes, and P_{ij} and P_{ijk} are circular permutation operators. To second order, the amplitude of the pairwise permutation is simply given by $J = 2t^2/U$, while the 3-site permutation appears at third order in perturbation theory with $K_3 = 6t^3/U^2$. The cases $\Phi = 0$ and $\Phi = \pi$ with purely real positive [32] and negative [33] three-site

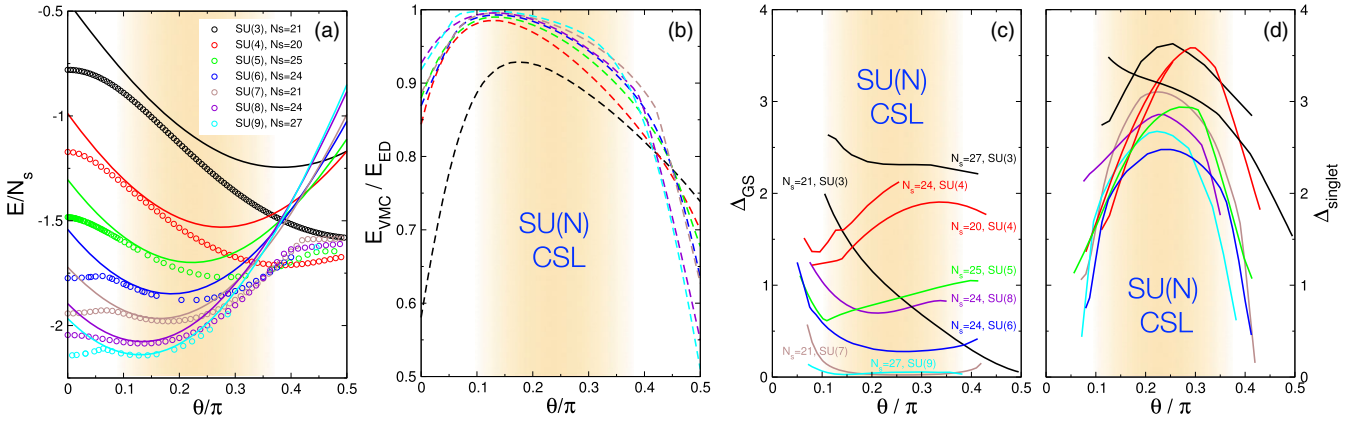

FIG. 1. Panel (a) Ground state energy per site as a function of θ for various N and N_s. Open symbols (full lines) denote ED (VMC) results. (b) Quality of the VMC wave function as measured by the ratio $E_{\mathrm{VMC}}/E_{\mathrm{ED}}$. (c) Energy splitting among the expected N singlet states forming the ground space manifold of a SU(N) CSL. (d) Energy gap from the ground state to the first excited singlet state which is not part of the expected ground space manifold.

permutation have been addressed earlier. In this Letter, we concentrate on the case of a purely imaginary three-site permutation $\Phi = \pi/2$ described by the Hamiltonian

$$H = \cos\theta \sum_{\langle i,j\rangle} P_{ij} + \sin\theta \sum_{(i,j,k)} (iP_{ijk} + \mathrm{H.c.}), \qquad (3)$$

with the parametrization $J = \cos\theta$ and $K_3 = \sin\theta$. We will discuss the experimental prospects of realizing this Hamiltonian towards the end of the Letter. It is interesting to note that parent Hamiltonians for SU(N) chiral spin liquids have been proposed recently [34,35]. While there are some structural similarities, it is not obvious that the spatially compact and physically more realistic Hamiltonian Eq. (3) features CSL phases. It is the goal of this Letter to provide compelling numerical evidence, based on large-scale exact diagonalizations (EDs) and Gutzwiller projected parton wave functions, that the above Heisenberg Hamiltonian indeed features extended regions of SU(N) CSLs for all values of $N = 3$ to 9 considered here.

Exact diagonalizations.—We start by investigating finite periodic triangular lattice clusters as a function of θ for various values of N. We focus on the range $\theta \in [0, \pi/2]$ in the following. $\theta > \pi/2$ is likely to be dominated by ferromagnetism, while $\theta < 0$ yields the time-reversed, but otherwise identical physics as $-\theta$. For small values of $N = 3, 4$ we used the standard ED approach employing all the space group symmetries, while only considering the individual color conservation, corresponding to an Abelian subgroup of SU(N). For all other N a recently developed ED approach by two of the authors [36], exploiting the SU(N) symmetry at the expense of spatial symmetries, is currently the only way to address these systems within ED. Depending on N, the largest system sizes N_s range from 21 to 27 lattice sites.

In Fig. 1(a) we plot the ED results for the energy per site of the ground state as a function of θ for all considered N (open symbols). While the curves for $N \lesssim 5$ look rather smooth at first sight, it is visible that the energy per site displays kinks around $\theta/\pi \sim 0.05 - 0.1$ and at $\theta/\pi \sim 0.35 - 0.4$ for $N = 6$ to 9. For comparison we plot the energy expectation value of parameter-free Gutzwiller projected CSL model wave functions for all values of N (full lines). We will discuss the properties of these wave functions in a moment. Interestingly, these model wave functions have very competitive energies, especially in the θ region slightly above the first kink. For a quantitative comparison we show in Fig. 1(b) the ratio of the variational energy divided by the ED ground state energy. It is impressive that for N beyond 3 the best ratio exceeds 0.98 for the system sizes considered. So the picture so far is that the small and large θ regimes for all considered N are most likely other phases, while the intermediate region could harbor CSLs.

SU(N) CSLs are intrinsically topologically ordered: They exhibit a nontrivial ground state degeneracy on the torus [27,37] and fractional excitations. The ground state degeneracy on the torus is expected to be N for these particular states with N different Abelian anyons [26,27]. In our numerical simulations, we can detect this degeneracy by investigating the low-energy spectrum on samples with a total number of lattice sites N_s that is an integer multiple of N. In Fig. 1(c) we display the energy spread Δ_{GS} of these N expected ground states for different N as a function of θ. As a general trend we observe that the splitting reduces significantly as we increase N. On the other hand, several samples still show a substantial splitting. Naively one would expect a simple exponential suppression of the splitting with system size; however, in the related context of fractional Chern insulators a more subtle dependence of the ground space splitting on the actual shape of the clusters has been observed and rationalized [48]. We think that similar considerations apply here as well.

Finally we also measure the gap Δ_{singlet} from the absolute ground state to the first singlet level that is not part of the expected ground state manifold. This is a measure for the excitation gap in the gapped CSL states. In Fig. 1(d), one observes an approximate dome-shaped behavior of this gap for all N, and furthermore this gap seems to depend only weakly on N. The approximate region in θ where the N-fold ground state degeneracy splitting is small compared to the excitation gap (for large N) is indicated as a shaded region in all the panels, and indicates a rough stability region for the SU(N) CSLs on the triangular lattice. One should note, however, that the precise extent of the CSLs for small N is an open question at this point.

Variational parton approach.—An appealing way to describe the SU(N) CSLs is to use a parton-based mean field approach [26,27,49–54], complemented with a Gutzwiller projection. The idea is to fractionalize the elementary spin degree of freedom into fermionic spinons (partons) with N colors. For an exact description, a dynamical gauge field needs to enforce the physical constraint of one fermion per site. At the mean-field level, however, it is sufficient to specify the band structure and filling of the fermionic spinons. In the SU(N) CSLs of interest here, the spinon band structure consists of N bands, where the lowest band is completely filled for all N colors and separated by a gap from the other bands. In addition, this band is required to have Chern number ± 1. For the triangular lattice we use a Hofstadter-type tight-binding Hamiltonian with a uniform flux of π/N per triangular plaquette [55], fulfilling the requirements on the band structure. This mean-field state can now be turned into a valid spin wave function by the application of an exact Gutzwiller projection, enforcing the presence of exactly one fermionic spinon per site. Such a wave function can be handled by variational Monte Carlo (VMC) techniques, and in particular one can easily calculate the energy of the Hamiltonian Eq. (3) on rather large lattices. The VMC energies displayed in Figs. 1(a) and 1(b) have been obtained this way [37].

The next question is how the VMC approach is able to account for the nontrivial ground state degeneracy on the torus. It turns out that by threading flux through the noncontractible loops around the torus, one is able to span an N-dimensional subspace of Gutzwiller projected wave functions, with almost identical local properties on finite lattices. From the viewpoint of topological order, this corresponds to a charge pumping procedure, where one cycles through the N different ground states by threading a different anyonic flux through the interior of the torus. These concepts have recently been explored in the context of SU(2) CSL on several lattices [56–58]. We have checked in Fig. 2 that the subspace of wave functions spanned by using 30 different boundary conditions at the mean-field level leads to a robust rank-N overlap matrix, therefore corroborating the expectation of an N-fold degenerate ground state manifold in the thermodynamic limit also at the VMC level.

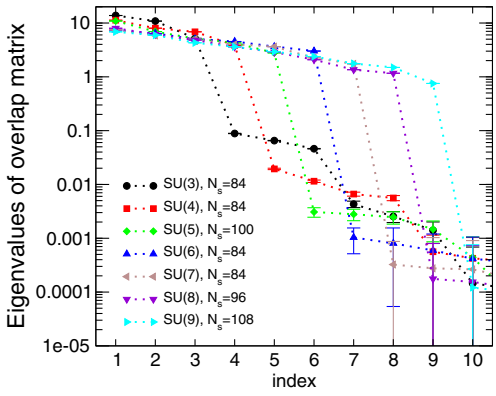

FIG. 2. VMC ground space degeneracy: ordered sequence of eigenvalues of the overlap matrix of Gutzwiller projected wave functions with 30 random values of threaded flux. The overlap matrix has precisely N large eigenvalues for an SU(N) CSL.

Since the variational energies for SU(3) turned out not to be very competitive, as shown in Figs. 1(a) and 1(b), we explicitly calculated the overlaps of individual ED eigenstates of the Hamiltonian Eq. (3) with the three orthogonal Gutzwiller wave functions obtained on the same system size. In Fig. 3 we plot the summed squared overlap of all three wave functions (area of filled circles) with the ED eigenstates (crosses) as a function of θ. Here we consider a $N_s = 12$ site system, where the momenta of the three ED ground states in the CSL phase are at the zone center (one) and at the corners of the Brillouin zone (twofold degenerate). Around $\theta = 0$, the SU(3) triangular lattice Heisenberg model is in a three-sublattice color ordered state [59,60]; however, in the region around $\theta/\pi \sim 0.25$, the three lowest ED eigenstates indeed have sizeable overlap

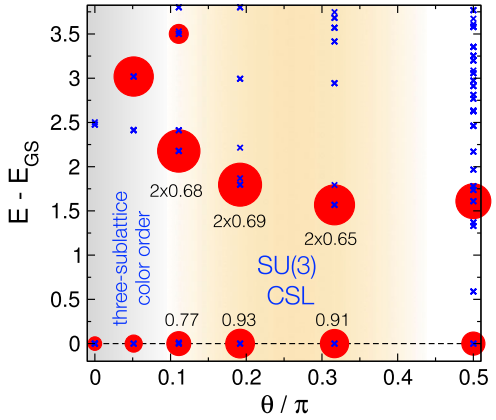

FIG. 3. Summed squared overlaps of the VMC model wave functions with ED eigenstates for $N = 3$ and $N_s = 12$. The blue crosses denote ED eigenstates, while the area of the filled red circles denotes the total squared overlap on those eigenstates. Around $\theta/\pi \approx 0.25$, the summed overlaps on the lowest three ED eigenstates (degeneracy $1 + 2$) account for over 75% of the total weight, while the ground state alone is at 90%.

with the VMC model wave functions, thereby underlining the presence of an SU(3) CSL for sufficiently large values of θ also for $N = 3$.

Edge states.—Another hallmark of chiral topological phases is the presence of chiral edge modes in the energy spectrum of systems with a boundary. It has been understood that the characteristic energy level structure of the edge excitations as a function of the momentum along the boundary serves as a fingerprint of the type of topological order realised in the bulk [61]. The SU(N) CSLs considered here are expected to exhibit a chiral edge energy spectrum described by the SU$(N)_1$ Wess-Zumino-Novikov-Witten (WZNW) conformal field theory (CFT) [27]. This is the same CFT that governs the low-energy spectrum of well-studied one-dimensional critical SU(N) spin chains [34,35,62,63].

In order to test this hypothesis numerically we choose to emulate a disk geometry by considering the specific $N_s = 19$ site triangular lattice with open boundary conditions depicted in the left panel of Fig. 4. Such a lattice might actually be built in future ultracold atom experiments with optical lattices and a tight confining potential. This sample still has a sixfold rotation axis about the central site, yielding an angular momentum quantum number which we use to plot the energy spectrum. The energy spectrum of the disc has no topological ground state degeneracy, but features gapless edge modes which typically propagate only in one direction. The precise multiplet structure of the edge modes depends on the anyonic sector. In our setup, this sector can be simply labeled as $a = (N_s \mod N)$. In Table I of the Supplemental Material [37], we have compiled the SU$(N)_1$ WZNW CFT predictions for the different irreducible representations of SU(N) which appear at a given excitation energy, here qualitatively labeled by the excess angular momentum $l - l_0$. In the remaining panels of Fig. 4 we display the actual ED energy spectrum of the Hamiltonian Eq. (3) for a fixed value of $\theta/\pi = 0.25$ for $N = 3$ up to 8 as a function of the angular momentum $l - l_0$. For all N one can clearly identify a branch of chiral excitations propagating to the right. The analytical predictions are indicated by the dimensions of the SU(N) irreducible representations. For all N the numerical data for the first three sectors ($l - l_0 = 0, 1, 2$) are in full agreement with the analytical predictions. The splitting between the multiplets at a given value of l is expected to vanish as N_s grows, and the spectrum should become linear with a certain edge state velocity. The observed structure of the edge excitations confirms the SU$(N)_1$ WZNW CFT predictions and thus strengthens the case for Abelian SU(N) CSLs in the model Hamiltonian Eq. (3).

Experimental considerations.—With the recent realization of the Mott-crossover regime in 3D optical lattices with fermionic Ytterbium atoms [64,65] the future for strongly correlated SU(N) quantum magnetism is shining bright. Our proposal for triangular lattices builds on ingredients that have been demonstrated separately: the possibility to realize Mott insulators in optical lattices, and to create static artificial gauge fields in an optical lattice (for alkaline atoms) [66,67]. Besides, working with the triangular lattice is a big advantage because the 3-site permutation term is the first and only term to appear to third order in perturbation theory starting from the Hubbard model with one particle per site, by contrast to, e.g., the square and honeycomb lattice, where they appear at order 4 and 6, respectively, and are not the first corrections. The chiral phase typically appears for $\theta \simeq 0.3$, which, using the perturbation expressions of $J = 2t^2/U$ and $K_3 = 6t^3/U^2$, corresponds to $t/U \simeq 0.1$. This might be small enough to be still in the

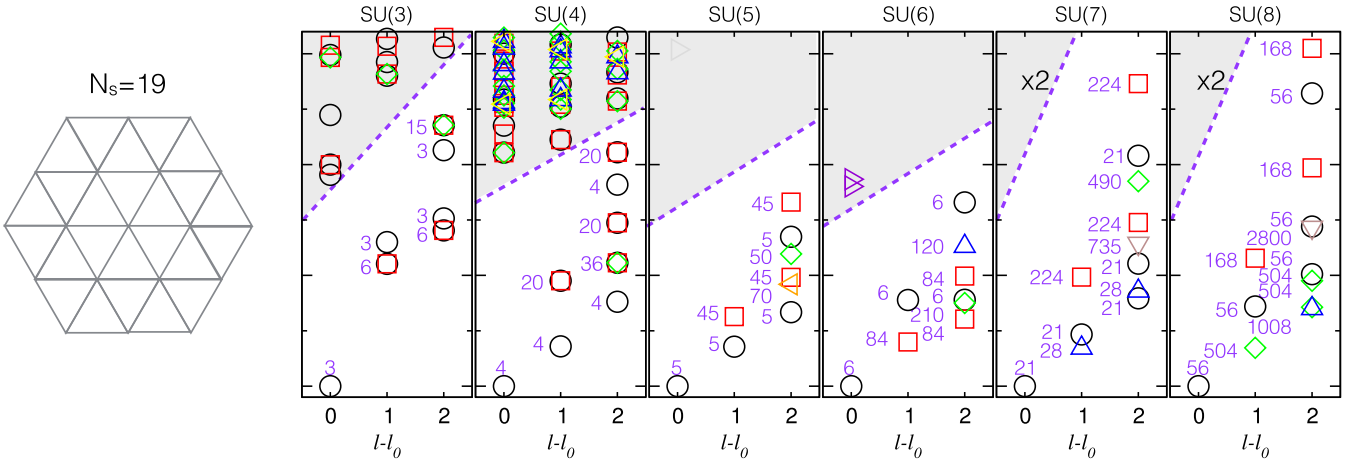

FIG. 4. Edge states in SU(N) CSLs: the leftmost panel displays the $N_s = 19$ site triangular cluster with open boundary conditions used. In the various other panels we exhibit the low energy spectrum as a function of the angular momentum around the central site (l_0 denotes the ground state angular momentum). The chiral edge states are clearly visible, with a characteristic SU(N) multiplet structure, which corresponds to a particular sector of a chiral $SU(N)_1$ Wess-Zumino-Novikov-Witten conformal field theory. The analytical predictions are indicated by the dimensions of the SU(N) multiplets and can be found in Table I of the Supplemental Material [37].

Mott insulating phase, and to ensure that higher order corrections are negligible. In future studies one might also relax the $\pi/2$ flux per plaquette condition, and explore the extent of the expected stability region of the SU(N) CSL phases.

Several interesting questions need to be addressed in future work. For example, is it possible to directly engineer the required three site exchange terms in Hamiltonian Eq. (3) using sophisticated quantum optics schemes? There is hope that the current activity on lattice gauge-theory implementations will bring techniques to address this question. Another intriguing question regards the detection of SU(N) CSL edge states in actual experiments, using for example spectroscopic techniques for small droplets or braiding protocols for the Abelian anyons [27].

The authors acknowledge P. Corboz, M. Hermele, T. Quella, A. Sterdyniak, H.-H. Tu, and Hongyu Yang for useful discussions. This work has been supported by the Swiss National Science Foundation, the JSPS KAKENHI Grant No. 2503802, the Hungarian OTKA Grant No. K106047, by the Austrian Science Fund FWF (F-4018-N23 and I-1310-N27/DFG-FOR1807), and by the National Science Foundation under Grant No. NSF PHY11-25915.

[1] D. S. Rokhsar and S. A. Kivelson, Phys. Rev. Lett. **61**, 2376 (1988).
[2] R. Moessner and S. L. Sondhi, Phys. Rev. Lett. **86**, 1881 (2001).
[3] A. Ralko, M. Ferrero, F. Becca, D. Ivanov, and F. Mila, Phys. Rev. B **71**, 224109 (2005).
[4] I. Affleck and J. B. Marston, Phys. Rev. B **37**, 3774 (1988).
[5] Y. Ran, M. Hermele, P. A. Lee, and X.-G. Wen, Phys. Rev. Lett. **98**, 117205 (2007).
[6] P. Corboz, M. Lajkó, A. M. Läuchli, K. Penc, and F. Mila, Phys. Rev. X **2**, 041013 (2012).
[7] V. Kalmeyer and R. B. Laughlin, Phys. Rev. Lett. **59**, 2095 (1987).
[8] X. G. Wen, F. Wilczek, and A. Zee, Phys. Rev. B **39**, 11413 (1989).
[9] X. G. Wen, Phys. Rev. B **40**, 7387 (1989).
[10] D. F. Schroeter, E. Kapit, R. Thomale, and M. Greiter, Phys. Rev. Lett. **99**, 097202 (2007).
[11] L. Messio, B. Bernu, and C. Lhuillier, Phys. Rev. Lett. **108**, 207204 (2012).
[12] S. Bieri, M. Serbyn, T. Senthil, and P. A. Lee, Phys. Rev. B **86**, 224409 (2012).
[13] Y.-C. He, D. N. Sheng, and Y. Chen, Phys. Rev. Lett. **112**, 137202 (2014).
[14] S.-S. Gong, W. Zhu, and D. N. Sheng, Sci. Rep. **4**, 6317 (2014).
[15] B. Bauer, L. Cincio, B. P. Keller, M. Dolfi, G. Vidal, S. Trebst, and A. W. W. Ludwig, Nat. Commun. **5**, 5137 (2014).
[16] C. Nayak, S. H. Simon, A. Stern, M. Freedman, and S. Das Sarma, Rev. Mod. Phys. **80**, 1083 (2008).
[17] C. Wu, J.-p. Hu, and S.-c. Zhang, Phys. Rev. Lett. **91**, 186402 (2003).
[18] C. Honerkamp and W. Hofstetter, Phys. Rev. Lett. **92**, 170403 (2004).
[19] M. A. Cazalilla, A. F. Ho, and M. Ueda, New J. Phys. **11**, 103033 (2009).
[20] A. V. Gorshkov, M. Hermele, V. Gurarie, C. Xu, P. S. Julienne, J. Ye, P. Zoller, E. Demler, M. D. Lukin, and A. M. Rey, Nat. Phys. **6**, 289 (2010).
[21] F. Scazza, C. Hofrichter, M. Höfer, P. C. De Groot, I. Bloch, and S. Fölling, Nat. Phys. **10**, 779 (2014).
[22] G. Pagano, M. Mancini, G. Cappellini, P. Lombardi, F. Schäfer, H. Hu, X.-J. Liu, J. Catani, C. Sias, M. Inguscio, and L. Fallani, Nat. Phys. **10**, 198 (2014).
[23] X. Zhang, M. Bishof, S. L. Bromley, C. V. Kraus, M. S. Safronova, P. Zoller, a. M. Rey, and J. Ye, Science **345**, 1467 (2014).
[24] M. A. Cazalilla and A. M. Rey, Rep. Prog. Phys. **77**, 124401 (2014).
[25] N. Read and S. Sachdev, Phys. Rev. Lett. **62**, 1694 (1989).
[26] M. Hermele, V. Gurarie, and A. M. Rey, Phys. Rev. Lett. **103**, 135301 (2009).
[27] M. Hermele and V. Gurarie, Phys. Rev. B **84**, 174441 (2011).
[28] G. Szirmai, E. Szirmai, A. Zamora, and M. Lewenstein, Phys. Rev. A **84**, 011611 (2011).
[29] G. Chen, K. R. A. Hazzard, A. M. Rey, and M. Hermele, Phys. Rev. A **93**, 061601 (2016).
[30] O. I. Motrunich, Phys. Rev. B **73**, 155115 (2006).
[31] D. Sen and R. Chitra, Phys. Rev. B **51**, 1922 (1995).
[32] H.-H. Lai, Phys. Rev. B **87**, 205111 (2013).
[33] H.-H. Lai, Phys. Rev. B **87**, 205131 (2013).
[34] H.-H. Tu, A. E. Nielsen, and G. Sierra, Nucl. Phys. **B886**, 328 (2014).
[35] R. Bondesan and T. Quella, Nucl. Phys. **B886**, 483 (2014).
[36] P. Nataf and F. Mila, Phys. Rev. Lett. **113**, 127204 (2014).
[37] See Supplemental Material at http://link.aps.org/supplemental/10.1103/PhysRevLett.117.167202 for further information concerning the variational Monte Carlo simulations, the analogy with the Quantum Hall effect, and the SU(N)$_1$ predictions for the chiral edge state. This includes Refs. [26,27,38–47].
[38] B. Halperin, Helv. Phys. Act. **56**, 75 (1983).
[39] Y. Hatsugai, K. Ishibashi, and Y. Morita, Phys. Rev. Lett. **83**, 2246 (1999).
[40] X. G. Wen, F. Wilczek, and A. Zee, Phys. Rev. B **39**, 11413 (1989).
[41] J.-W. Mei and X.-G. Wen, Phys. Rev. B **91**, 125123 (2015).
[42] Y. Zhang, T. Grover, and A. Vishwanath, Phys. Rev. Lett. **107**, 067202 (2011).
[43] Y. Zhang, T. Grover, A. Turner, M. Oshikawa, and A. Vishwanath, Phys. Rev. B **85**, 235151 (2012).
[44] Y. Zhang and A. Vishwanath, Phys. Rev. B **87**, 161113 (2013).
[45] P. Corboz, M. Lajkó, A. M. Läuchli, K. Penc, and F. Mila, Phys. Rev. X **2**, 041013 (2012).
[46] T. Li and F. Yang, Phys. Rev. B **81**, 214509 (2010).
[47] J.-W. Mei and X.-G. Wen, arXiv:1407.0869.
[48] A. M. Läuchli, Z. Liu, E. J. Bergholtz, and R. Moessner, Phys. Rev. Lett. **111**, 126802 (2013).

[49] G. Baskaran, Z. Zou, and P. Anderson, Solid State Commun. **63**, 973 (1987).
[50] G. Baskaran and P. W. Anderson, Phys. Rev. B **37**, 580 (1988).
[51] I. Affleck, Z. Zou, T. Hsu, and P. W. Anderson, Phys. Rev. B **38**, 745 (1988).
[52] E. Dagotto, E. Fradkin, and A. Moreo, Phys. Rev. B **38**, 2926 (1988).
[53] X.-G. Wen and P. A. Lee, Phys. Rev. Lett. **76**, 503 (1996).
[54] T. Senthil and M. P. A. Fisher, Phys. Rev. B **62**, 7850 (2000).
[55] Note that at this stage the flux per plaquette is unrelated to the flux per plaquette in the original Fermi-Hubbard Hamiltonian Eq. (1).
[56] Y. Zhang, T. Grover, and A. Vishwanath, Phys. Rev. B **84**, 075128 (2011).
[57] H.-H. Tu, Y. Zhang, and X.-L. Qi, Phys. Rev. B **88**, 195412 (2013).
[58] A. Wietek, A. Sterdyniak, and A. M. Läuchli, Phys. Rev. B **92**, 125122 (2015).
[59] A. Läuchli, F. Mila, and K. Penc, Phys. Rev. Lett. **97**, 087205 (2006).
[60] B. Bauer, P. Corboz, A. M. Läuchli, L. Messio, K. Penc, M. Troyer, and F. Mila, Phys. Rev. B **85**, 125116 (2012).
[61] X. G. Wen, *Quantum Field Theory of Many-Body Systems: From the Origin of Sound to an Origin of Light and Electrons* (Oxford University Press, Oxford, 2004).
[62] B. Sutherland, Phys. Rev. B **12**, 3795 (1975).
[63] I. Affleck, Nucl. Phys. **B265**, 409 (1986).
[64] S. Taie, R. Yamazaki, S. Sugawa, and Y. Takahashi, Nat. Phys. **8**, 825 (2012).
[65] C. Hofrichter, L. Riegger, F. Scazza, M. Höfer, D. R. Fernandes, I. Bloch, and S. Fölling, Phys. Rev. X **6**, 021030 (2016).
[66] M. Aidelsburger, M. Atala, M. Lohse, J. T. Barreiro, B. Paredes, and I. Bloch, Phys. Rev. Lett. **111**, 185301 (2013).
[67] H. Miyake, G. A. Siviloglou, C. J. Kennedy, W. C. Burton, and W. Ketterle, Phys. Rev. Lett. **111**, 185302 (2013).